

The Internal Wave Action Model IWAM

Peter Müller and Andrei Natarov

Department of Oceanography, University of Hawaii, Honolulu, HI 96822

Abstract. This article describes the overall modeling strategy for the Internal Wave Action Model (IWAM), which is a hybrid dynamical model that predicts the internal wave field in a basin or region for given forcing and environmental fields. Large-scale internal tides and near-inertial internal waves will be modeled by integrating appropriate hydrodynamic equations. Intermediate and small-scale internal waves will be modeled by integrating the radiative balance equation (RBE). The RBE describes changes of the action density spectrum along wave group trajectories as a result of forcing, interaction, and dissipation processes; RBE makes the random phase, geometric optics (WKB), and weak interaction approximations. The action density spectrum is a reduced description of the internal wave field; it is a statistical second-order moment from which all other second-order moments can be calculated. IWAM will combine different dynamical processes into a coherent framework. Methodologically, it is similar to the WAM model developed by the surface wave modeling community. One important task in constructing IWAM is specifying the source terms in the radiation balance equation. The specification of the dissipation source function is discussed in some detail. It involves the “derivation” of a functional form with free parameters and solutions of the RBE for the reflection off a straight slope, where propagation and dissipation are assumed to balance. Comparisons with observations and numerical process studies then allow the calibration of the free parameters. The calibration and validation of the RBE are the first tasks in constructing IWAM. The next tasks include the integration of the radiative balance equations and embedding it into a circulation model. The major issues and problems are discussed.

Introduction

Sufficient progress in internal wave theory and observation has been made to attempt the construction of a dynamical internal wave model. Here we describe one such modeling effort: the hybrid Internal Wave Action Model (IWAM). Large-scale internal tides and near-inertial internal waves will be modeled by integrating appropriate hydrodynamic equations in an ocean basin or a region. Intermediate- and small-scale internal waves will be modeled by integrating the radiative balance equation (RBE). Together, these components will predict the internal wave field in a basin or a region for given forcing and environmental fields. Specifically, IWAM will

- provide understanding of the internal wave field as a balance of generation, transfer, and dissipation processes,

- predict changes in the internal wave field in response to changes in forcing and environmental fields, and
- determine internal wave induced stresses, fluxes, mixing, and dispersion.

Overall, IWAM is expected to focus research on internal wave dynamics, similar to the way that the introduction of the Garrett and Munk model spectrum focused research on internal wave kinematics. Eventually, IWAM is envisioned to be run in conjunction with circulation, turbulence, tracer, population, and acoustic models where it will provide the internal-wave-induced fluxes, transports, dispersion, mixing, noise, and internal wave environment.

In this article we first reiterate some of the reasons that motivate the construction of a dynamical internal wave model. Chief among these reasons are the link

between internal waves and diapycnal mixing, the possible role of internal waves (IW) in cascading energy from large to small scales, and important processes such as acoustic propagation and biological production that are affected by IW. We then briefly discuss some relevant aspects of the kinematics of IW. One must distinguish between near-inertial IW, internal (or baroclinic) tides, the IW continuum, and nonlinear waves such as solitons and bores. These different kinds of IW will be modeled differently. Our current dynamical understanding of open ocean IW is reviewed next. Internal waves are generated as large-scale near-inertial IW by the atmosphere and as large-scale internal tides by the barotropic tide at topography. These large-scale waves propagate in physical space while nonlinear wave-wave interactions and other scattering processes cascade their energy through wavenumber space to small scales where they break and dissipate. The generation and propagation of the large-scale near-inertial IW and internal tides will be modeled by integrating appropriate hydrodynamic equations on a spatial grid. The cascade through the internal-wave continuum will be modeled by integrating the radiative balance equation (RBE). The RBE is a reduced description. It foregoes deterministic information and describes the evolution of the energy (or action) density spectrum, a statistical second order moment of the IW field from which all other second order moments can be calculated. The RBE makes the random phase, geometric optics (WKB), and weak interaction approximations. Central to the RBE are the source terms representing the various dynamical processes. These source terms can be “derived” from underlying hydrodynamical equations under more or less restrictive assumptions. Some of these derivations contain free parameters that must be calibrated by observations or results from numerical process studies. As an explicit example we describe in some detail the construction of the dissipation source function. We conclude with a discussion of the major issues and problems facing the IWAM modeling effort.

Motivation

There are many reasons to study and understand oceanic internal waves. Here we point out the link between IW and diapycnal mixing, the possible participation of IW in the overall energy cascade from the large generation scales to the small dissipation scales, and the effect of IW on acoustic propagation.

Diapycnal mixing. The link between diapycnal mixing and IW is by now well established (e.g., Müller and Briscoe, 2000). Diapycnal mixing is an integral factor in the meridional overturning circulation of the ocean. The slow upwelling in the ocean interior across

density surfaces requires counteracting diapycnal diffusion. Diapycnal diffusion in a stably stratified fluid requires mechanical energy, and the availability of this energy might well be the controlling factor in setting the strength of the overturning circulation as, e.g., discussed by *Munk and Wunsch* (1998). It has been found that

- Diapycnal mixing in the ocean interior is driven by intermittent patches of small-scale turbulence.
- The turbulent patches have a vertical extent of up to a few meters and are caused by breaking internal waves.
- Internal waves break by either shear or convective instabilities that are caused by chance superpositions or encounters with critical layers.

Diapycnal mixing can also be caused by other processes such as double diffusion. The link between IW and diapycnal mixing has come out of wave-wave interaction theories (*McComas and Müller*, 1981; *Henye* *et al.*, 1986) and has led to parameterizations of the diapycnal mixing coefficient or turbulent dissipation rate in terms of the internal wave shear and strain. Different schemes have been suggested (*Gregg*, 1989; *Henye* *et al.*, 1991; *Wijesekera et al.*, 1993; *Polzin et al.*, 1995; *Sun and Kunze*, 1999; *Gregg et al.*, 2003) and are currently being used to estimate the diapycnal mixing coefficient or turbulent dissipation from ADCP or CTD measurements; an example is given in Figure 1. Thus, by understanding and predicting internal waves we may understand and predict diapycnal mixing.

Routes to dissipation. The general circulation of the ocean is forced by surface fluxes of momentum, heat, and fresh water at large, basin-wide horizontal scales of the order of 1000 km and at long time-scales of the order of 1 year and longer. The circulation has comparable large and long scales, as well as intermediate ones associated with equatorial zonal and lateral boundary currents and various mesoscale instabilities. In steady state, the large scale input of variance into the velocity, temperature, and salinity fields of the circulation must be dissipated at small scales by molecular friction, heat conduction, and salt diffusion. For molecular friction the dissipation scale is the Kolmogorov scale, of the order 10^{-2} m. We presently do not know by which processes the variances cascade across the eight orders of magnitude separating the generation and dissipation scales.

For the kinetic energy - the variance of the velocity field - the first steps in the down-scale cascade are the processes of barotropic and baroclinic instability. These

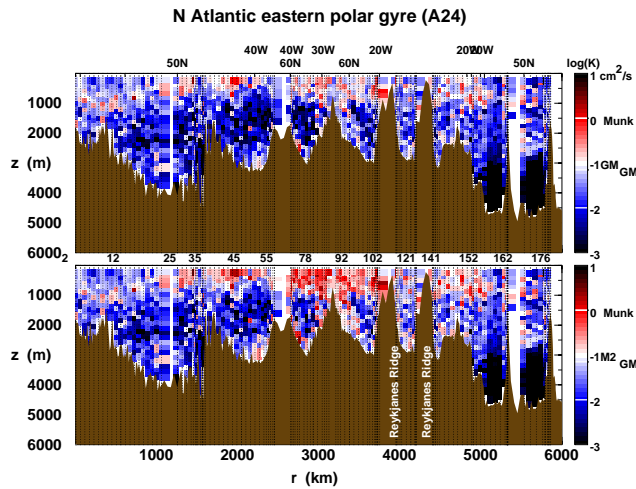


Figure 1. Eddy diffusivity K inferred from internal wave strain using the *Gregg et al.* (2003) parameterization. The data are from one of the WOCE/ACCE A24 cruises in the eastern polar gyre of the N. Atlantic with multiple crossings of the Mid-Atlantic and Reykjanes Ridges. Strain is inferred from CTD profile segments, either from buoyancy frequency squared or potential temperature gradient. The upper panel assumes a shear/strain ratio of 3 (corresponding to the GM model value) while the lower panel uses a semidiurnal shear/strain ratio under the assumption that internal tides may be important. The latter increases with latitude so that high-latitude diffusivities in the lower panel are higher than those at low latitude. For both panels, white values correspond to expectations for a typical (GM) internal wave field, blue values are lower, red values are higher. (Courtesy of E. Kunze)

generate mesoscale eddies with a spatial scale of the order of the internal Rossby radius of deformation, which is about 50 km on average. These instabilities thus provide a forward (downscale) cascade of energy from basin-wide generation scale to the internal deformation radius. But any further down-scale cascade is inhibited by the fact that mesoscale eddies, like the general circulation, are very anisotropic flows, constrained by rotation and stratification to be nearly horizontal (i.e., to be nearly two-dimensional in this sense). These motions approximately satisfy hydrostatic and geostrophic momentum balances, and their evolution is governed by the potential vorticity equation. The key point in the present context is that the advective dynamics of such balanced motions - called geostrophic turbulence - exhibits a forward or down-scale cascade of enstrophy (i.e., variance of potential vorticity) to its dissipation at small scales but an inverse (up-scale) turbulent cascade of energy toward larger scales, hence away from dissipation

by molecular viscosity at small scales (Charney, 1971); this behavior is analogous to 2D turbulence, i.e., the turbulence in a two-dimensional fluid. Thus balanced dynamics do not provide an efficient root to energy dissipation in the ocean interior.

At smaller scales, stratified shear flows are known to become unstable, due to Kelvin-Helmholtz instability, once the Richardson number falls below $1/4$. This instability is observed to set in at vertical scales of about 10 m. This instability starts a downscale energy cascade - called stratified turbulence - where the overturning eddies work against buoyancy forces, mix the water column, and increase the potential energy at the same time as they are being dissipated by molecular friction. Once the down-scale cascade reaches the Osmidov or buoyancy scale, which is of the order of 1 m, the stratification becomes unimportant and the turbulence becomes a three-dimensional, isotropic turbulence that efficiently cascades energy down-scale through a Kolmogorov inertial range to the dissipation scales.

As depicted in Figure 2, there is thus a gap of roughly three orders of magnitude between the anisotropic, balanced motions at large scales and the isotropic, small-scale motions that complete the forward energy cascade to dissipation. This gap needs to be bridged for an equilibrium kinetic energy balance in the ocean. Figure 2 depicts three possible routes:

- the internal gravity wave route (II)
- the instability route (III), and
- the boundary route (IV)

The internal wave route assumes that pre-existing internal gravity waves interact with large- and mesoscale motions and catalyze a cascade of their energy to small scales. This and the other routes are more fully discussed in *Müller et al.* (2003). None of these routes to dissipation, or any other route, have strong theoretical or observational confirmation yet. But it is essential that we determine and understand the routes to dissipation. Simply inserting horizontal and vertical eddy viscosity coefficients in models of the oceanic general circulation and tuning their values to some desired outcome is hazardous and diminishes the fidelity of the model. Any circulation model that aspires to predictive capabilities must base its parametrizations on a dynamical understanding of the parameterized motions. Internal waves are part of these parameterized motions—perhaps a crucial part.

Acoustic propagation. The sound speed c is the most fundamental quantity that determines acoustic propa-

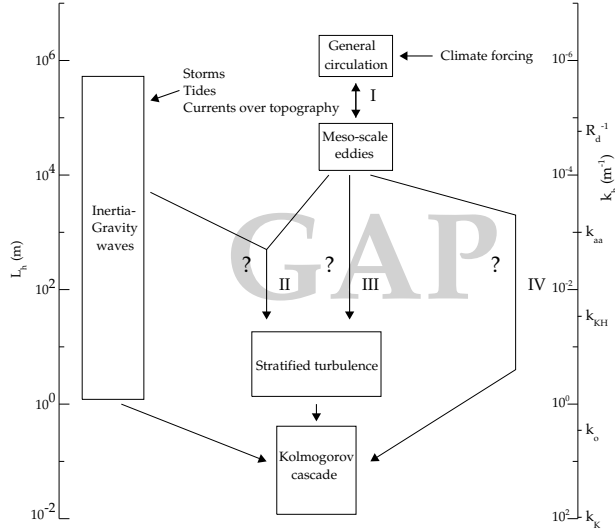


Figure 2. Possible energy pathways of the general circulation. Energy must be transferred across the gap between large-scale balanced flows and small-scale imbalanced flows that exhibit a forward cascade towards viscous dissipation. I. Baroclinic/barotropic instability. II. Interaction with inertia-gravity waves. III. Unbalanced instabilities. IV. Dissipation in boundary layers. (From Müller *et al.*, 2003)

gation. It is defined by the thermodynamic relation

$$c^{-2} = \frac{\partial \rho(p, \theta, s)}{\partial p} \quad (1)$$

where $\rho(p, \theta, s)$ is the equation of state, i.e., the density of sea water as a function of pressure p , potential temperature θ , and salinity s . The sound speed increases with pressure, temperature and salinity. The effect of salinity is relatively small. In the ocean, pressure, potential temperature, and salinity are functions of position \mathbf{x} and time t . So is the sound speed

$$c(\mathbf{x}, t) = c(p(\mathbf{x}, t), \theta(\mathbf{x}, t), s(\mathbf{x}, t)) \quad (2)$$

The sound speed at a specific horizontal position and a specific time as a function of the vertical or depth coordinate z is called a sound speed profile $c(z)$. The gradient of the sound speed profile is given by

$$\frac{dc}{dz} = \left(\frac{\partial c}{\partial \theta} \right)_{p,s} \frac{d\theta}{dz} + \left(\frac{\partial c}{\partial s} \right)_{p,\theta} \frac{ds}{dz} + \left(\frac{\partial c}{\partial p} \right)_{\theta,s} \frac{dp}{dz} \quad (3)$$

The first two terms constitute the potential gradient

$$\left(\frac{dc}{dz} \right)_p = \left(\frac{\partial c}{\partial \theta} \right)_{p,s} \frac{d\theta}{dz} + \left(\frac{\partial c}{\partial s} \right)_{p,\theta} \frac{ds}{dz} \quad (4)$$

The third term is called the adiabatic gradient. Internal gravity waves - and often other oceanic motions - cause surfaces of constant sound speed to move up and down and not to be level in space. An internal wave of vertical displacement ζ thus causes a change in the sound speed given to first order by

$$\delta c = - \left(\frac{dc}{dz} \right)_p \zeta \quad (5)$$

The sound speed variation δc enters the acoustic wave equation and affects acoustic propagation. The forward or direct problem is to calculate the acoustic field for given internal wave displacements. The inverse problem consists of inferences about ζ from acoustic measurements. Internal wave velocities \mathbf{u} also affect acoustic propagation, through a Doppler shift

$$\delta c = \mathbf{k} \cdot \mathbf{u} \quad (6)$$

The effect is small and generally ignored, except in reciprocal transmissions where the difference in transmission times is related to the water velocity along the acoustic ray path.

Kinematics

Free linear gravity waves have frequencies between the Coriolis frequency f and the buoyancy or Brunt-Väisälä frequency N . In the ocean their vertical scales range from about 1 km (first baroclinic mode) to 10 m, and horizontal scales range from tens of kilometers to tens of meters. Since internal waves are dispersive, there can also exist nonlinear waves of permanent form, where nonlinear steepening is balanced by dispersion. There exist different kinds of such nonlinear waveforms, including bores and solitons. In the ocean such nonlinear waves are formed when internal tides shoal and steepen as they propagate onto the shelf. Figure 3 shows a frequency spectrum of the horizontal kinetic energy. The spectrum shows a peak near the inertial frequency f , another peak at the semidiurnal tidal frequency M_2 and a broad continuum with a -2 slope. The continuum is often well described by the model spectrum of *Garrett and Munk* (1972). The GM spectrum, as it is now called, describes a wavefield that is horizontally isotropic (waves coming in from all horizontal directions equally) and vertically symmetric (as many waves propagate upward as downward). Often upward and downward propagating waves are assumed to be phase-locked and to produce vertically standing “normal modes.” The most surprising and significant aspect of the GM spectrum is its universality. To observe significant (say larger than a factor of three) deviations from the GM spectrum one has to go to very

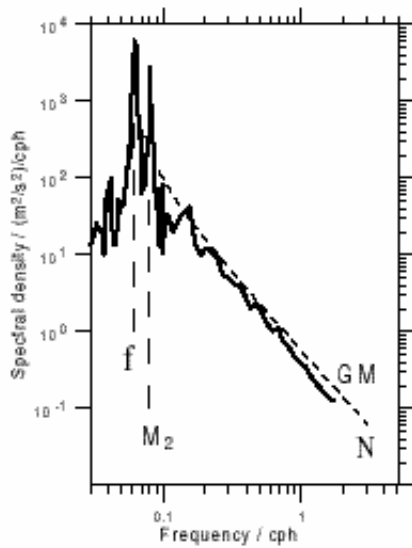


Figure 3. Frequency spectrum of the horizontal kinetic energy at 140 m depth at a site in the northeast Pacific during the Ocean Storms Experiment, 1987-88. Internal waves exist between the Coriolis frequency f and the buoyancy frequency N . M_2 is the semi-diurnal tidal frequency. The dashed line labeled GM is the Garrett and Munk model prediction (Courtesy of M. Levine).

special places such as the Arctic Ocean or submarine canyons. The dashed line in Figure 3 represents the GM spectrum and shows how well the observed continuum is represented by it. The GM spectrum does not account for the variance in the internal (or baroclinic) tidal peaks, which contain a considerable but highly variable fraction of the variance. The GM spectrum also does not properly represent many of the observed features of the inertial peak. It neither reflects its large temporal variability, nor its strong dependence on depth, nor its vertical asymmetry (most near-inertial IW are observed to propagate downward). The modeling strategy of IWAM will take these differences in the kinematic structure into account. It will treat separately

- the large scale near-inertial waves and large scale internal tides,
- the internal wave continuum, and
- nonlinear soliton- or bore-like internal waves.

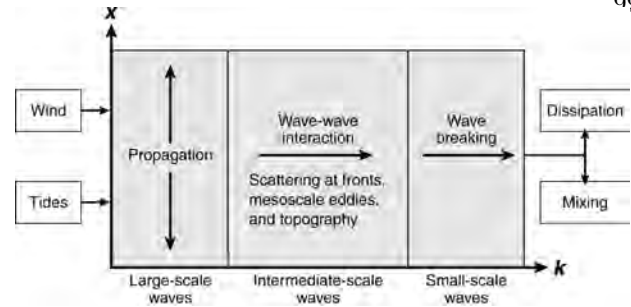


Figure 4. The conventional dynamic balance of the oceanic internal wave field in physical (x) and wavenumber (k) space. The wind and tides generate large-scale waves of near inertial and tidal frequencies. These large-scale waves propagate away from their sources in physical space and cascade towards small-scale waves in wavenumber space. The cascade is caused by wave-wave interactions and scattering at fronts, mesoscale eddies, topography and other scatterers. The small-scale waves break and cause turbulence and mixing.

Dynamics

The conventional dynamic balance is depicted in Figure 4. It has only two energy sources for internal waves:

- changes in the atmospheric windstress cause inertial oscillations in the oceanic surface mixed layer; part of their energy propagates into the ocean interior as large-scale, near-inertial internal waves,
- barotropic (or surface) tidal currents flowing across topography in a stratified ocean generate internal waves of tidal frequency, the baroclinic tides. Their large-scale components propagate into the ocean interior.

There is good observational evidence for both these generation processes. Near-inertial internal waves have been observed to propagate away from the surface underneath storm and cyclone tracks and quantitative estimates of the energy input are becoming available (*D'Asaro, 1985; Alford, 2001 and 2003; Watanabe and Hibiya, 2002*). Baroclinic tidal beams have been observed to emanate from certain topographic features and can often be traced for hundreds of kilometers (*Ray and Mitchum, 1997; Dushaw et al., 1995*) and quantitative estimates of the energy input are again becoming available (*Sjöberg and Stigebrandt, 1992; Morozov, 1995; Egbert and Ray, 2000 and 2001; St-Laurent and Garrett, 2002*).

As these large-scale waves propagate away from their generation region, they are assumed to interact nonlinearly with themselves and other internal waves and

to scatter at mesoscale eddies, fronts, and topography. These nonlinear interaction and scattering processes transfer energy out of the large-scale waves into ever smaller scale waves that eventually break and cause turbulence and mixing. In a breaking event, the wave energy is partly converted to potential energy, since the mixing of a stably stratified fluid increases its potential energy.

Overall modeling strategy

Internal waves have horizontal scales down to tens of meters, vertical scales down to meters, and time scales down to tens of minutes. To adequately resolve IW one thus would have to integrate some appropriate hydrodynamic equation on a grid with horizontal spacing $\Delta x, \Delta y = O(10 \text{ m})$ and vertical spacing $\Delta z = O(1 \text{ m})$ with a time step $\Delta t = O(1 \text{ min})$. This is possible in a box of the order of $10 \text{ km} \times 10 \text{ km} \times 1 \text{ km}$ but is clearly beyond present and foreseeable future computer capabilities for regions or basins. Various “box” studies have been carried out to study specific processes.

Large-scale IW can be and have been resolved basin-wide and regionally. *Niwa and Hibiya* (2001) studied the generation and propagation of near-inertial IW in the North Pacific in a model with horizontal grid spacing of $1/6^\circ$ (18.5 km), 28 vertical levels, and 16-min time steps. The generation and propagation of internal tides has been modeled by *Xing and Davies* (1998), *Holloway* (2001), *Merrifield et al.* (2001), and *Merrifield and Holloway* (2002), among others. *Johnson et al.* (2003) studied the scattering of the internal tide at bottom topography in a region southwest of the Hawaiian Island chain.

To include into these basin-wide and regional models intermediate and small-scale IW not only requires exorbitant computer resources but also details in the forcing and environmental fields (e.g., topography) that are generally not available. However, this point can be turned to one’s advantage. All the detailed unresolved influences tend to randomize the phases of the waves. Because of all these unaccountable influences one can employ the random phase approximation. It assumes that the phases of the waves are random and that the only predictable quantity is the amplitude or energy of the wave, which is proportional to the amplitude squared. Instead of describing the IW field by its velocity vector, vertical displacement, and pressure, one thus describes the internal wave field by its energy density spectrum $E(\mathbf{k})$ which gives the distribution of wave energy among different wavenumbers. All other second-order moments of the IW field can be inferred from the energy density spectrum $E(\mathbf{k})$ by using IW kinematic relations.

A second property of the IW field also ought to be exploited to reduce the computational load: its near linearity. IW are by definition a nearly linear phenomenon. When the nonlinearities become large the field turns into stratified turbulence. The zeroth order physics of nearly linear internal wave is energy propagation along wave group trajectories. This zeroth order physics does not need to be calculated, wasting computer resources, but should be presupposed. Any modeling effort should assume (rather than calculate) that IW propagate along their trajectories. This assertion leads to the radiation balance equation discussed next.

Radiative balance equation

The radiative balance equation makes three basic approximations:

- the random phase approximation,
- the WKB or geometric optics approximation, and
- the weak interaction approximation.

The random phase approximation assumes that the various dynamical processes affecting the wave field will distort the wave phases in an irregular way such that it is neither possible nor useful to predict wave phases. Instead, the wave field is described by its energy or action density spectrum.

The WKB approximation assumes that the wavelengths of the waves are small compared to the scales of environment. The action density spectrum as a function of wavenumber then varies slowly with position and time on the scales of the environment.

The weak interaction approximation assumes that internal waves are basically a linear phenomenon. The waves propagate along their group trajectories, being only slowly modified by dynamical processes. The dynamical evolution of the action density spectrum along wave group trajectories is caused by generation, transfer, and dissipation processes.

How good are these approximations? The random phase approximation has worked well for the kinematic description of oceanic internal waves, except for some internal tide phenomena which are driven by and phase-locked to surface tide.

The weak interaction approximation holds well for most generation and transfer processes. It can even be expected to hold for processes such as wave breaking that are strongly nonlinear but localized in space. These processes are “weak-in-the-mean” in that they only cause moderate changes in the spectrum.

The WKB approximation is not a real problem but more a matter of definition. The environmental fields

are divided into a mean component with scales larger than the wavelengths in which waves propagate in WKB fashion and a fluctuating component with scales comparable to wavelengths at which the waves are scattered.

Because the radiation balance equation does not carry any wave phase information and assumes (as opposed to calculates) wave propagation it can eventually be integrated globally or regionally with a horizontal resolution of $\Delta x = O(100 \text{ km})$. This is different from direct numerical simulation (DNS) or large eddy simulation (LES) of internal waves in which phase information is retained and wave propagation is calculated. These studies have grid sizes of order $\Delta x = 1 \text{ cm}$ (DNS) or of order $\Delta x = 1 \text{ m}$ (LES) if they correctly interpret their diffusion coefficients as molecular coefficients or as representing the transfer across Kolmogorov's inertial range. There are of course studies that purport to simulate internal waves at a coarser resolution by introducing an eddy diffusion coefficient. These studies, however, assume that the high Reynolds number oceanic flow field can be simulated by a low Reynolds number model, an unsupported assumption so far.

Formally, the radiative balance equation takes the form (Müller and Olbers, 1975)

$$\begin{aligned} \left(\partial_t + \dot{\mathbf{x}} \cdot \partial / \partial \mathbf{x} + \dot{\mathbf{k}} \cdot \partial / \partial \mathbf{k} \right) A(\mathbf{k}, \mathbf{x}, t) \\ = S_{gen} + S_{trans} + S_{diss} \end{aligned} \quad (7)$$

where $A(\mathbf{k}, \mathbf{x}, t)$ is the action density spectrum, \mathbf{k} is the wavenumber vector, \mathbf{x} is the position vector, and t the time. The frequency of the waves can be obtained from the dispersion relation

$$\omega = \Omega(\mathbf{k}, \mathbf{x}, t) \quad (8)$$

which depends on the local values of the mean environmental fields which in turn depend in a slowly varying manner on position \mathbf{x} and time t . The wave group trajectories are defined by the group velocity

$$\mathbf{v} = \dot{\mathbf{x}} = \partial \Omega / \partial \mathbf{k} \quad (9)$$

and by the rate of refraction

$$\mathbf{r} = \dot{\mathbf{k}} = -\partial \Omega / \partial \mathbf{x} \quad (10)$$

The left-hand side of the radiation balance equation describes changes of the action density spectrum along wave trajectories. These changes are given by the dynamical source terms on the right hand side where S_{gen} describes the generation of internal wave action, S_{trans} the transfer of action across the spectrum, and S_{diss} the dissipation of wave action. Without any dynamical sources or sinks the action density spectrum does

not change along wave group trajectories. The radiation balance equation has to be augmented by boundary conditions.

Generally, the radiation balance equation becomes less accurate as the scales of the waves increase. The exact scale where the statistical description and the radiation balance equation need to be replaced by a deterministic description and hydrodynamic equations has not yet been determined. The radiation balance equation is clearly not applicable to tidally generated solitary waves propagating away from their generation sites.

Source terms

An important task is the specification of the source terms in the radiation balance equation and its boundary conditions. Some of these source terms can be derived from the basic hydrodynamic equations by making appropriate assumptions. Some examples are considered in this section. For highly nonlinear processes such as wave breaking, such a derivation is not possible. Instead one only arrives at functional forms with free parameters. These parameters must then be calibrated by comparing solutions of the RBE with observations or process simulations. This approach is demonstrated for the dissipation source function in the next section.

Reflection off a straight slope. At rigid boundaries the hydrodynamic boundary condition for inviscid flows is $\mathbf{u} \cdot \mathbf{n} = 0$ where \mathbf{u} is the velocity vector and \mathbf{n} is the normal vector of the boundary. The normal velocity component must be zero. For internal waves this condition gets transformed into reflection laws. One part of these laws relates the wavenumber and frequency of the reflected wave to those of the incident wave; the frequency and tangential wavenumber do not change upon reflection

$$\omega^r = \omega^i \quad (11)$$

$$k_t^r = k_t^i \quad (12)$$

The normal component of the reflected wavenumber can then be inferred from the "dispersion" relation

$$k_n^r = k_n(k_t^r, \omega^r) \quad (13)$$

Explicit formulas can be found in Eriksen (1982). Since the frequency does not change, the angle of the wave rays with respect to the vertical axis remains the same, rather than with respect to the normal vector. When this angle and the bottom slope add up to $\pi/2$ then the reflection becomes critical. The reflected wavenumber becomes infinite. The second part of the reflection laws determines the amplitude of the reflected

wave. Under the assumptions of the radiation balance equation it becomes

$$\mathbf{n} \cdot (\mathbf{F}_i + \mathbf{F}_r) = 0 \quad (14)$$

where

$$\mathbf{F}_{i,r} = \mathbf{v}(\mathbf{k}_{i,r}) E(\mathbf{k}_{i,r}) \quad (15)$$

is the energy flux of the incident and reflected wave. The normal energy flux must be zero at the boundary. Equation (14) provides the boundary conditions for the radiative balance equation.

Nonlinear wave-wave interactions. The hydrodynamic equations contain advective nonlinearities of the form $\mathbf{u} \cdot \nabla \psi$ where ψ is any of the prognostic variables. Under various weak interaction assumptions these nonlinearities lead to resonant wave-wave interactions. The general theory was developed by Hasselmann and Zakharov and first applied to internal waves by *Olbers* (1976) and *McComas and Bretherton* (1977). Subsequent investigations of nonlinear interactions among internal waves are reviewed in *Müller et al.* (1986). New analyses are pursued by *Lvov and Tabak* (2003). For internal waves, wave-wave interactions take the form of triad interactions. Two waves \mathbf{k}_1 and \mathbf{k}_2 interact to generate a third wave \mathbf{k}_3 . The source term in the RBE equation takes the form

$$S_{nl}(\mathbf{k}) = \int \int d^3\mathbf{k}' d^3\mathbf{k}'' T(\mathbf{k}, \mathbf{k}', \mathbf{k}'') A(\mathbf{k}') A(\mathbf{k}'') \quad (16)$$

where $T(\mathbf{k}, \mathbf{k}', \mathbf{k}'')$ is a transfer function that can be calculated from the underlying hydrodynamic equations. The source term describes the time rate of change of the action density spectrum at wavenumber \mathbf{k} . Wave action is gained at \mathbf{k} due to the interaction of waves \mathbf{k}' and \mathbf{k}'' that generate waves at \mathbf{k} . Wave action is lost at \mathbf{k} due to the interaction of waves \mathbf{k} and \mathbf{k}' that generate waves at \mathbf{k}'' . The double integral sums over all these possible interactions. The transfer function contains two delta functions because the triad interactions satisfy the resonant conditions

$$\omega = \omega' + \omega'' \quad (17)$$

$$\mathbf{k} = \mathbf{k}' + \mathbf{k}'' \quad (18)$$

The six-dimensional integral thus reduces to an integral over two-dimensional resonant surfaces.

The structure of the source terms for various other processes has been derived in *Müller and Olbers* (1975). Attempts have been made to evaluate some of these source terms for quasi-realistic conditions to assess the importance of the underlying process for the overall dynamics of IW. Such studies include the scattering of IW at bottom topography (*Müller and Xu*, 1992).

In a series of papers, *Polzin* (2003a,b) represents the nonlinear source function as a flux through wavenumber space. The functional form of the flux is based on a combination of theoretical and dimensional arguments with free parameters constrained by observations. The flux is toward high wavenumbers and assumed to be “dissipated.” This form is then utilized to calculate solutions of the radiation balance equation for the IW field above rough topography in the Brazil Basin, where IW generated by currents across topography propagate upward and flux their energy across the spectrum to dissipation.

Dissipation source function

Dissipation of internal wave energy is assumed to occur by wave breaking. Internal waves break by either shear or convective instabilities that are caused by either chance superposition or encounter of critical layers. Breaking internal waves not only generate turbulence but they mix the water column. Part of the IW energy is thus converted into potential energy. The energy in the turbulence is partly dissipated into heat and partly emitted as small-scale IW waves as the turbulent patch collapses and spreads laterally. Wave breaking is a highly nonlinear, localized, and sporadic process which has defied so far any rigorous derivation of the associated source function. However, its localized and sporadic nature in space and time makes it a process that is “weak-in-the-mean,” meaning that although the process itself is strongly nonlinear its effect on the overall spectrum is weak. This fact, together with the requirement that the source function must be negative, implies that the dissipation source function must have the form

$$S_{diss}(\mathbf{k}) = -\gamma A(\mathbf{k}) \quad (19)$$

boundary where the dissipation coefficient γ depends on wavenumber \mathbf{k} and integral properties of the wave field, such as the total energy, shear, or inverse Richardson number Ri^{-1} (*Hasselmann*, 1974, *Komen et al.*, 1994). Thus

$$\gamma = \gamma(\mathbf{k}, Ri^{-1}) \quad (20)$$

and 19 is only quasi-linear. To arrive at a more specific form *Natarov and Müller* (2003) proceeded as follows. First they assumed a separable functional form for the dissipation coefficient

$$\gamma(\mathbf{k}, Ri^{-1}) = c(\mathbf{k}) f(Ri^{-1}) \quad (21)$$

where the function $c(\mathbf{k})$ describes the wavenumber distribution of dissipation and the function $f(Ri^{-1})$ describes the intensity of dissipation, increasing with increasing inverse Richardson number. This functional form contains as a limit the *Garrett and Gilbert* (1988) scenario where all energy fluxed past a certain critical

wavenumber is instantaneously dissipated. The functions $c(\mathbf{k})$ and $f(Ri^{-1})$ need to be calibrated by observations or process simulations. To do so Natarov and Müller considered reflection of an incoming GM spectrum at a straight slope. Because of critical reflection, the reflected spectrum has (infinitely) high shear and inverse Richardson number with associated vigorous wave breaking. The dominant balance in RBE for the reflected spectrum can thus be assumed to be between propagation and dissipation. Hence

$$v_n(\mathbf{k}) \frac{\partial}{\partial x_n} A(\mathbf{k}, x_n) = -c(\mathbf{k}) f(Ri^{-1}) A(\mathbf{k}, x_n) \quad (22)$$

where x_n is the coordinate normal to the slope and v_n the group velocity in the normal direction. This equation is subject to the condition

$$A(\mathbf{k}, x_n = 0) = A_r(\mathbf{k}) \quad (23)$$

where $A_r(\mathbf{k})$ is the reflected spectrum obtained from the prescribed incoming GM spectrum. A solution can be obtained if the contribution to the inverse Richardson number from the incoming spectrum is neglected. This is indeed a good approximation since the incoming GM spectrum carries only little shear. The solution is facilitated by the fact that the function $f(Ri^{-1})$ can be separated from the problem by introducing a scaled distance $\xi = \xi(x_n)$ such that

$$\frac{d\xi}{dx_n} = f(Ri^{-1}) \quad (24)$$

The RBE then reduces to the linear form

$$v_n(\mathbf{k}) \frac{\partial}{\partial \xi} A(\mathbf{k}, \xi) = -c(\mathbf{k}) A(\mathbf{k}, \xi) \quad (25)$$

which is solved by

$$A(\mathbf{k}, \xi) = A(\mathbf{k}, \xi = 0) \exp \left\{ -\frac{c(\mathbf{k})}{v_n(\mathbf{k})} \xi \right\} \quad (26)$$

If $c(\mathbf{k})$ is known one can calculate from this solution

$$Ri^{-1}(\xi) = \int d^3\mathbf{k} w(\mathbf{k}) A(\mathbf{k}, \xi) \quad (27)$$

where $w(\mathbf{k})$ is a known weighting function. Comparing this solution to observations (or results from process studies)

$$Ri^{-1}(\xi) = Ri_{obs}^{-1}(x_n) \quad (28)$$

then yields $\xi = \xi(x_n)$ and hence $f(Ri^{-1})$. Conversely, if $\xi = \xi(x_n)$ is known one can solve equation (25) for $c(\mathbf{k})$ and substitute observations (or results of process studies). The result is

$$c(\mathbf{k}) = -\frac{v_n(\mathbf{k})}{c(\mathbf{k})} \log \frac{A^{obs}(\mathbf{k}, \xi)}{A^{obs}(\mathbf{k}, \xi = 0)} \quad (29)$$

The right hand side of this equation needs to be independent of x_n . This provides a test of the validity of the assumptions that went into the derivation. Of course, the solutions for $f(Ri^{-1})$ and $c(\mathbf{k})$ have to be found simultaneously, requiring some iterative solution technique. Also, the complete action density spectrum as a function of wavenumber vector and distance x_n is not observed, nor easily calculable in process simulations. Generally, only moments like the energy density, inverse Richardson number and dissipation rate are observed. One thus assumes functional forms for $c(\mathbf{k})$ and $f(Ri^{-1})$ with a certain number of free parameters, calculates the observed fields (the forward problem) and then determines the free parameters by minimizing the “distance” between these calculated fields and the observed fields (the inverse problem). Details are forthcoming in *Natarov and Müller* (A dissipation function for IWAM, submitted, 2003).

Initial tasks and outlook

The construction of IWAM requires a variety of tasks. The major ones are these:

- the determination, evaluation, calibration and validation of the source terms of the radiative balance equation,
- the integration of the radiative balance equation, and
- the embedding of the radiation balance equation into a high resolution circulation model.

The first step of the first task is the determination of the source terms. Most of the source terms in the RBE can be and have been “derived” from the hydrodynamic equations under more or less restrictive assumptions. Some of these “derivations” contain free parameters that need to be calibrated. The source terms often have a fairly complicated form. The wave-wave interaction source term is an integral over a two-dimensional resonance surface. Efficient algorithms need to be designed or approximations and simplifications be implemented. Such approximations and simplifications are also necessary when the source term requires information about environmental fields that is not readily available. Scattering at bottom topography depends on the bottom spectrum which is not everywhere available at the relevant wavenumbers.

The second step is the calibration and validation of the source terms by comparison with observations or numerical process studies. This should be done in circumstances where only a limited number of processes dominate the RBE and where transparent solutions of the

RBE can be obtained. This step is envisioned to be a very productive and fruitful basic research phase, since it will allow us to explicitly test dynamical balances underlying various sets of observations. Examples include tests of whether the decay of internal tides or near-inertial IW is due to dissipation, nonlinear wave-wave interaction, bottom scattering, or any other process, or the identification of the processes by which a spectrum reflected off topography adjusts. Comparisons of solutions of the RBE with results from numerical process studies will allow us to determine the range of validity of the RBE approach and its calibration. Overall, this phase will encode the knowledge that we have from observational and numerical process studies into the radiation balance equation.

The second task is to put all processes together and integrate the radiation balance. While the WAM project for surface waves is a precedent for this task it should be emphasized that the internal wave problem constitutes a propagation problem in a six-dimensional phase space (three space coordinates and three wavenumber components) whereas the surface-wave problem is a four-dimensional problem. Straightforward extension of the 4D to the 6D problem exceeds current computer capacities and ways need to be explored that reduce the computational load. The third task is to embed the RBE model in a circulation model. Again, there is precedence from WAM.

All these tasks are challenging, theoretically, observationally, and computationally, but not unsurmountable. The result of the efforts will be a model that determines the state of the internal wave field from the governing physics.

Acknowledgments. Work on the development of IWAM has been supported by the Office of Naval Research.

References

- Alford, M. H., Improved global maps and 54-year history of wind-work on ocean inertial motions, *Geophys. Res. Lett.*, *30*(8), 10.1029/2002GL016614, 2003.
- Alford, M. H., Internal swell generation: The spatial distribution of energy flux from the wind to mixed layer near-inertial motions. *J. Phys. Oceanogr.*, *31*, 2359–2368, 2001.
- Charney, J. G., Geostrophic turbulence. *J. Atmos. Sci.*, *28*, 1087–1095, 1971.
- D’Asaro, E. A., The energy flux from the wind to near-inertial motions in the surface mixed layer. *J. Phys. Oceanogr.*, *15*, 1043–1059, 1985.
- Dushaw, B. D., B. D. Cornuelle, P. F. Worcester, B. M. Howe, and D. S. Luther, Barotropic and baroclinic tides in the central North Pacific Ocean determined from long-range reciprocal acoustic transmissions. *J. Phys. Oceanogr.*, *25*, 631–647, 1995.
- Egbert, G. A., and R. D. Ray, Significant dissipation of tidal energy in the deep ocean inferred from satellite altimeter data. *Nature*, *45*, 775–778, 2000.
- Egbert, G. A., and R. D. Ray, Estimates of M_2 tidal energy dissipation from TOPEX Poseidon altimeter data. *J. Geophys. Res.*, *106*, 22475–22502, 2001.
- Eriksen, C. C., Observations of internal wave reflection off sloping bottoms. *J. Geophys. Res.*, *87*, 525–538, 1982.
- Garrett, C. J. R., and W. H. Munk, Space-time scales of internal waves. *Geophys. Fluid Dyn.*, *2*, 225–264, 1972.
- Garrett, C., and D. Gilbert, 1988: Estimates of vertical mixing by internal waves reflected off a sloping bottom. In *Elsevier Oceanog. Series*, J. C. J. Nihoul and B. M. Jamart Edrs., *46*, 405–423, 1988.
- Gregg, M. C., Scaling turbulent dissipation in the thermocline. *J. Geophys. Res.*, *94*, 9686–9698, 1989.
- Gregg, M. C., T. B. Sanford and D. P. Winkel, Reduced mixing from the breaking of internal waves in equatorial ocean waters. *Nature*, *422*, 513–515, 2003.
- Hasselmann, K., On the spectral dissipation of ocean waves due to white capping. *Boundary Layer Met.*, *6*, 107–127, 1974.
- Henye, F. S., Scaling of internal wave prediction for ϵ , in *Dynamics of Internal Gravity Waves in the Ocean*, Proc. ‘Aha Hulihoa’ a Hawaiian Winter Workshop, Honolulu, HI, U of Hawaii, 11–13 Jan 1991. P. Müller and D. Henderson, Eds., 233–236, 1991.
- Henye, F. S., J. Wright and S. M. Flatté, Energy and action flow through the internal wave field - An eikonal approach. *J. Geophys. Res.*, *91* (C7), 8487–8495, 1986.
- Holloway, P. E., A regional model of the semidiurnal internal tide on the Australian North West Shelf. *J. Geophys. Res.*, *106* (C9), 19,625–19,638, (2000JC000675), 2001.
- Johnston, T. M. S., M. A. Merrifield, and P. E. Holloway, Internal tide scattering at the Line Islands Ridge, *J. Geophys. Res.*, submitted, 2003.
- Komen, G.J., L. Cavaleri, M. Donelan, K. Hasselmann, S. Hasselmann, P.A.E.M. Janssen, *Dynamics and Modelling of Ocean Waves*. Cambridge University Press, 532 pp., 1994.
- Lvov, Y., and E. Tabak, A Hamiltonian Formulation and the Garrett-Munk spectrum of internal waves in the ocean, submitted to *J. Fluid Mech.*, 2003.
- McComas, C. H. and F. P. Bretherton, Resonant interaction of oceanic internal waves. *J. Geophys. Res.*, *82*, 1397–1412, 1977.

- McComas, C. H., and P. Müller, The dynamic balance of internal waves. *J. Phys. Oceanogr.*, *11*, 970-986, 1981.
- Merrifield, M. A., P. E. Holloway, and T. M. S. Johnston, The generation of internal tides at the Hawaiian Ridge, *Geophys. Res. Lett.*, *28*, 559-562, 2001.
- Merrifield, M. A., and P. E. Holloway, Model estimates of M_2 internal tide energetics at the Hawaiian Ridge. *J. Geophys. Res.* *107* (C8), 10.1029/2001JC000996, 2002.
- Morozov, E. G., Semidiurnal internal wave global field, *Deep-Sea Res.* *42*, 135-148, 1995.
- Müller, P., and D. J. Olbers, On the dynamics of internal waves in the deep ocean. *J. Geophys. Res.*, *80*, 3848-3860, 1975.
- Müller, P., G. Holloway, F. Henyey, and N. Pomphrey, Nonlinear interactions among internal gravity waves. *Rev. Geophys.*, *24*, 493-536, 1986.
- Müller, P. and N. Xu, Scattering of oceanic internal gravity waves off random bottom topography. *J. Phys. Oceanogr.*, *22*, 474-488, 1992.
- Müller, P. and M. G. Briscoe, Diapycnal Mixing and Internal Waves. *Oceanography*, *13*, 98-103, 2000.
- Müller, P., J. McWilliams, and J. Molemaker, Routes to dissipation. The 2D/3D turbulence conundrum. In: *Marine Turbulence*. Cambridge University Press (accepted), 2003.
- Munk, W., and C. Wunsch, Abyssal recipes II: energetics of tidal and wind mixing. *Deep-Sea Res.*, *45*, 1997-2010, 1998.
- Niwa, Y., and T. Hibiya, Numerical study of the spatial distribution of f the M_2 internal tide in the Pacific Ocean. *J. Geophys. Res.*, *106* (C10), 22,441-22,449, 2001.
- Olbers, D. J., Nonlinear energy transfer and the energy balance of the internal wave field in the deep ocean. *J. Fluid Mech.*, *74*, 375-399, 1976.
- Polzin, K. L., J. M. Toole, and R. W. Schmitt, Finescale parameterization of turbulent dissipation. *J. Phys. Oceanogr.*, *25*, 306-328, 1995.
- Polzin, K. L., A heuristic description of internal wave dynamics. *J. Phys. Oceanogr.*, (in press), 2003a.
- Polzin, K.L., Idealized solutions for the energy balance of the finescale internal wavefield, *J. Phys. Oceanogr.*, (in press), 2003b.
- Ray R., and G. T. Mitchum, Surface manifestation of internal tides in the deep ocean: Observations from altimetry and island gauges. *Prog. Oceanogr.*, *40*, 135-162, 1997.
- St. Laurent, L., and C. Garrett, The role of internal tides in mixing the deep ocean. *J. Phys. Oceanogr.*, *32*, 2882-2899, 2002.
- Sjöberg, B., and A. Stigebrandt, Computations of the geographical distribution of the energy flux to mixing processes via internal tides and the associated vertical circulation in the ocean. *Deep-Sea Res.*, *39* (2), 269-291, 1992.
- Sun, H., and E. Kunze, Internal wave/wave interactions: Part II. Spectral energy transfer and turbulence production. *J. Phys. Oceanogr.*, *29*, 2905-2919, 1999.
- Watanabe, M., and T. Hibiya, Global estimates of the wind-induced energy flux to inertial motions in the surface mixed layer, *Geophys. Res. Lett.*, *29*, 80.1-80.4, 10.1029/2001GL014422, 2002.
- Wijesekera, H. W., L. Padman, T. Dillon, M. Levine, C. Paulson, and R. Pinkel, The application of internal-wave dissipation models to a region of strong forcing, *J. Phys. Oceanogr.*, *23*, 269-286, 1993.
- Xing, J., and A. M. Davies, A three-dimensional model of internal tides on the Malin-Hebrides shelf and shelf edge. *J. Geophys. Res.*, *103*, 27,821-27,847, 1998.

This preprint was prepared with AGU's L^AT_EX macros v4, with the extension package 'AGU++' by P. W. Daly, version 1.6b from 1999/08/19.

